

TECHNICAL ADVANCE

An alternative tandem affinity purification strategy applied to Arabidopsis protein complex isolation

Vicente Rubio¹, Yunping Shen^{1,2}, Yusuke Saijo¹, Yule Liu¹, Giuliana Gusmaroli¹, Savithramma P. Dinesh-Kumar¹ and Xing Wang Deng^{1,*}

¹Department of Molecular, Cellular, and Developmental Biology, Yale University, New Haven, CT 06520-8104, USA, and

²Peking-Yale Joint Research Center of Plant Molecular Genetics and Agrobiotechnology, College of Life Sciences, Peking University, Beijing 100871, China

Received 28 October 2004; accepted 26 November 2004.

*For correspondence (fax +1 203 432 5726; e-mail xingwang.deng@yale.edu).

Summary

Tandem affinity purification (TAP) strategies constitute an efficient approach for protein complex purification from many different organisms. However, the application of such strategies for purifying endogenous Arabidopsis multi-protein complexes has not yet been reported. Here, we describe an alternative TAP (TAPa) system that successfully allows protein complex purification from Arabidopsis. In our newly generated TAPa tag we have replaced the tobacco etch virus (TEV) protease cleavage site with the more specific and low-temperature active rhinovirus 3C protease site. In addition, the second purification step can now be performed through two different affinity tags: a six His repeat or nine copies of a myc repeat. To examine our purification procedure we generated a C-terminal fusion between the TAPa tag and CSN3, a component of the multi-protein COP9 signalosome (CSN) complex. Subsequent analysis showed that CSN3-TAPa could rescue a *csn3* mutant, and that the components of the CSN complex could be co-purified with CSN3-TAPa. As part of our long running interest in light signaling in Arabidopsis we have generated Arabidopsis transgenic lines harboring, both N-terminal and C-terminal TAPa fusions of many different light signaling pathway regulators. Molecular characterization of these transgenic lines showed fusion expression in 88% of the genes analyzed and that this expression is largely independent of the fusion orientation. Mutant complementation analysis showed that most of the TAPa fusions analyzed retained function of the wild-type proteins. Taken together, the data demonstrate the suitability of the TAPa system to allow efficient multi-protein complex isolation from stably transformed Arabidopsis.

Keywords: TAP, CSN, CSN3, protein complex purification, protein tagging, Arabidopsis.

Introduction

Since Rigaut *et al.* (1999) described the tandem affinity purification (TAP) system and its use to purify protein complexes from yeast, a number of studies have arisen in recent years demonstrating the applicability of such a system in many other different organisms. TAP-purified protein complexes have been isolated from bacteria (Gully *et al.*, 2003), mammalian cells (Knuesel *et al.*, 2003), insect cells (Forler *et al.*, 2003) and tobacco leaves (Rohila *et al.*, 2004). The simplicity, high yield, speed and reliability of this method, combined with recent improvements in mass spectrometry techniques, make it an ideal strategy for

high-throughput protein complex component identification (Graumann *et al.*, 2004; Puig *et al.*, 2001). In addition, the TAP system allows protein isolation under native conditions, therefore allowing functional studies in which the activity or post-translational modifications on one protein or protein complex can be examined (Puig *et al.*, 2001).

Although the TAP system has been recently applied to plant protein complex isolation in a transient expression system (Rohila *et al.*, 2004), so far, a purification procedure applied to stably transformed transgenic lines harboring a TAP-tagged protein has not been reported. Such an

approach would allow the molecular and functional characterization of the TAP fusion in a whole plant context, as well as purification of proteins under physiological conditions. In addition, the effects on the protein complex composition, modifications and activity due to a wider range of growth conditions, stimuli, and plant material used during purification, could be assessed.

We have generated a modified TAP tag in which we have replaced the original tobacco etch virus (TEV) protease cleavage site with the sequence recognized by the more specific and low-temperature active human rhinovirus 3C (3C) protease. The original calmodulin binding protein (CBP) domain has been replaced by a six histidine (6xHis) and a nine myc (9xmyc) repeat in the second affinity purification step. In contrast to the original TAP strategy, all the steps in our purification procedure can be performed efficiently at 4°C which should allow a more stable complex isolation. In addition, final elution does not require EDTA-containing buffers, which should help to keep the integrity of certain complexes as well as the activity of cation-dependent enzymes such as metalloproteases.

Arabidopsis transgenic lines expressing the COP9 signalosome (CSN) subunit CSN3 fused to our modified TAP tag have been generated and subjected to molecular and functional characterization. CSN is a highly conserved multi-protein complex consisting of eight subunits (CSN1–8) which plays a key role in the ubiquitin/26S proteasome proteolytic regulatory pathway (Deng *et al.*, 2000; Serino and Deng, 2003; Wei *et al.*, 1994, 1998). CSN interacts with the Skp1-cullin-F-box (SCF) E3 ubiquitin ligase and promotes RUB1 (Related to Ubiquitin 1; also known as Nedd8 in mammals) deconjugation (derubylation) of cullins (Cope *et al.*, 2002; Lyapina *et al.*, 2001; Schwechheimer *et al.*, 2001; Zhou *et al.*, 2001). Other activities related to CSN include the control of nucleocytoplasmic partitioning of key factors such as the plant photomorphogenesis negative regulator COP1 or the human cyclin-dependent kinase inhibitor p27^{kip1} (Chamovitz *et al.*, 1996; Tomoda *et al.*, 1999). In addition, a CSN-mediated deconjugation of ubiquitin peptides (deubiquitination) from target proteins or polyubiquitin chains has been reported (Groisman *et al.*, 2003; Zhou *et al.*, 2003). The CSN-dependent derubylation of cullins and protein deubiquitination activities require the metalloprotease domain present in the CSN5 subunit (Cope *et al.*, 2002; Groisman *et al.*, 2003; Lyapina *et al.*, 2001). Plants depleted in any of the CSN subunits show CSN complex disorganization, accumulation of rubylated cullin 1 (CUL1) and lethal *fusca* phenotype characterized by accumulation of anthocyanins and constitutive photomorphogenic features (reviewed in Serino and Deng, 2003). The extensive knowledge on composition, structure and activities, and the availability of antibodies against each subunit make the CSN an ideal candidate to validate our purification procedure.

In this paper we show that the Arabidopsis CSN complex can be isolated from plant extracts by TAP purification of a tagged CSN3 subunit. In addition, we have generated transgenic plant lines containing TAP fusions with 31 proteins involved in light signaling and the ubiquitin/26S proteasome pathway. The expression levels of the fusion proteins have been examined and, in some cases, a functional study has been carried out using mutant phenotype complementation analysis. The data presented in this study demonstrate the suitability of our TAP system for protein complex isolation from Arabidopsis tissues in a high-throughput manner.

Results

TAPa tags, vectors and strategy

We constructed N-terminal and C-terminal TAP tags composed of two copies of the immunoglobulin-binding domain of protein A from *Staphylococcus aureus* (2xlgG-BD), a human rhinovirus 3C (3C) protease cleavage site, a six histidine repeat (6xHis) and nine myc epitopes (9xmyc) (Figure 1a). Both TAP tags were cloned into binary vectors containing two copies of the cauliflower mosaic virus 35S promoter (2x35S) and a tobacco mosaic virus U1 Ω sequence. The latter is a translational enhancer which acts similarly to a 5'-CAP and a polyA tail and recruits eIF4F to increase translation from an mRNA (Gallie, 2002). The cloning of genes into these vectors was facilitated by including GATEWAY based-recombination sites (GATEWAY; Invitrogen, Carlsbad, CA, USA) in both N-terminal and C-terminal expression cassettes. A Nos terminator (Nos ter) sequence was present at the 3' end of both expression cassettes (Figure 1b).

As previously described (Rigaut *et al.*, 1999), our TAP strategy consists in two affinity purification steps separated by a specific-protease cleavage (Figure 2). The first affinity purification step takes advantage of the 2xlgG-BD present in the tagged protein to perform affinity purification using IgG coated-beads. For subsequent elution we used 3C protease instead of the original TEV protease. Contrary to TEV protease, whose lowest efficient cleavage temperature is 16°C, 3C protease allows very efficient cleavage at 4°C. In addition, 3C protease is more specific than TEV as its cleavage site consists of an eight amino acid sequence (Figure 1a) instead of a six amino acid sequence as with TEV protease. In the second affinity purification step, the original CBP was replaced with a 6xHis and a 9xmyc repeat. Therefore, the second step can be performed now using, alternatively, metal affinity chromatography or specific myc epitope immunoaffinity purification.

As the new tags we generated and the purification protocol we established differed notably from those described in the TAP strategy, we named our system as alternative tandem affinity purification (TAPa).

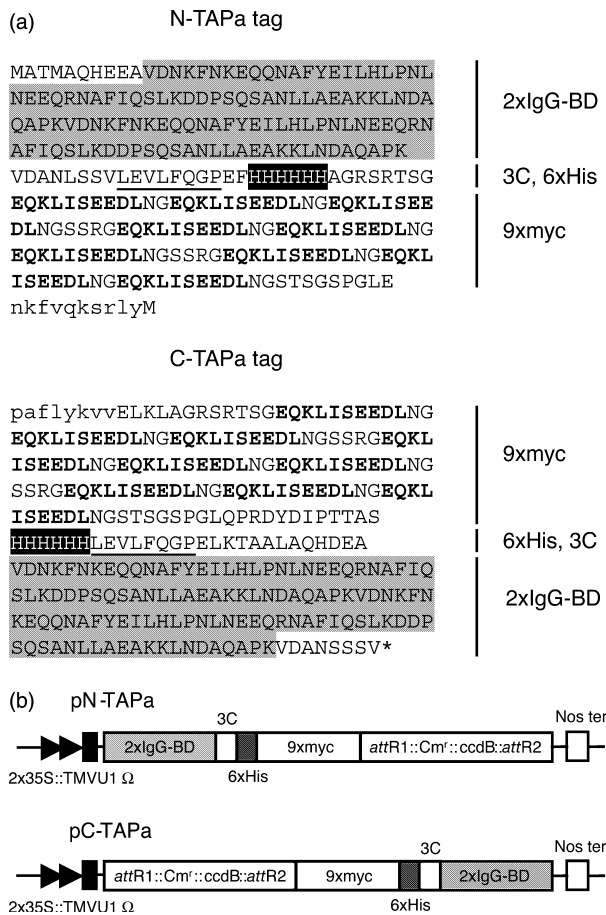


Figure 1. TAPa tag sequence and expression cassette structure.

(a) Amino acid sequence of the TAPa tags. The sequence corresponding to the two copies of the protein A IgG binding domain is highlighted in gray in both N-terminal and C-terminal TAPa tags. The six histidine repeat is highlighted in black. The sequence for the 3C protease cleavage site is underlined. Each one of the nine repeats of the myc epitope is shown in bold characters. The GATEWAY *attB1* (in the N-TAPa tag) and the *attB2* (in the C-TAPa tag) sequences are shown in lower case. An asterisk corresponds to the stop codon for the C-terminal fusion. In the N-TAP tag, the first Met for the tagged protein is designated as a capital M at the end of the *attB1* sequence. The N-TAPa and C-TAPa tag peptide sequences contain 293 and 307 residues, respectively.

(b) Diagrammatic representation of the expression cassettes in TAPa vectors. Both pN-TAPa and pC-TAPa vectors allow translational fusion, N-terminal and C-terminal, respectively, of proteins of interest to the TAPa tag. The expression is driven by two copies of the cauliflower mosaic virus 35S promoter (2x35S) and a tobacco mosaic virus (TMV) U1 Ω translational enhancer. The TAPa tag consists of two copies of the protein A IgG binding domain (2xIgG-BD), an eight amino acid sequence corresponding to the 3C protease cleavage site (3C), a six histidine stretch (6xHis), and nine repeats of the myc epitope (9xmyc). Both pN-TAPa and pC-TAPa vectors contain GATEWAY cloning sites (*attR1::Cm^r::ccdB::attR2*). A Nos terminator (Nos ter) sequence is located downstream of each expression cassette.

Functional and molecular characterization of CSN3-TAPa transgenic lines

The CSN is a 550-kDa conserved multi-protein complex which consists of eight subunits (CSN1–8) ranging in size

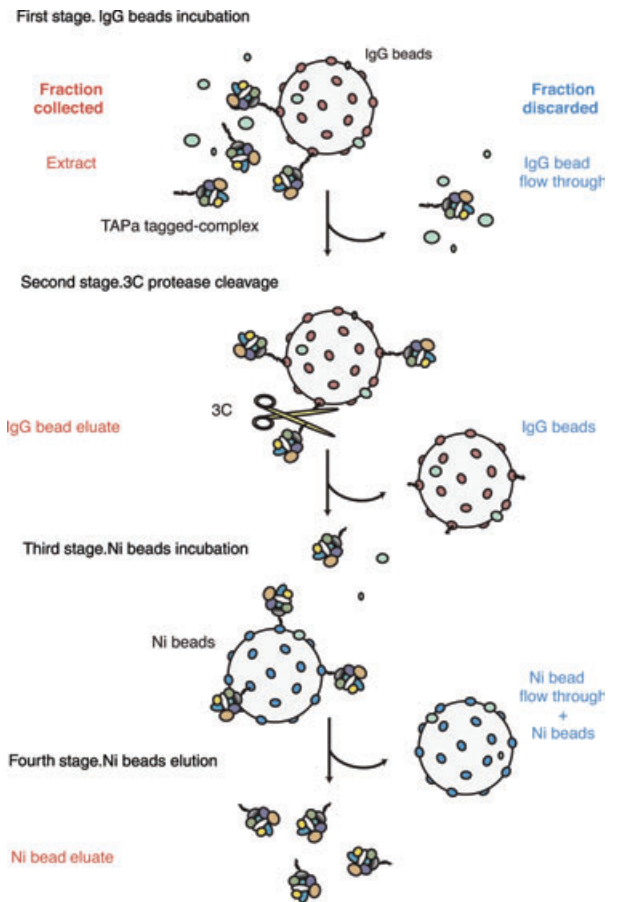


Figure 2. Schematic representation of the TAPa purification procedure.

Four different stages are shown. (1) Protein extracts are incubated with IgG beads in the first affinity purification step. (2) Elution of TAPa-tagged proteins involves specific cleavage on the TAPa tag by the low-temperature active rhinovirus 3C protease (3C). (3) The next affinity purification step consists of the incubation of IgG beads eluates with Ni beads or, alternatively, with α -myc beads. (4) Elution of proteins from beads is variable and depends on the final purpose (0.05 M imidazole-containing buffers might be employed when using Ni beads). Fractions collected during every step in the procedure are depicted in red. Flow through fractions and beads discarded after each step are shown in blue.

from 57 kDa (CSN1) to 22 kDa (CSN8) (Deng *et al.*, 2000; Serino and Deng, 2003; Wei *et al.*, 1994, 1998). As CSN composition, structure and activities are well characterized and, in addition, antibodies against all Arabidopsis CSN subunits have been generated, we chose the CSN complex to validate our purification procedure using the TAPa strategy. With this aim, we generated transgenic lines containing a C-terminal fusion of the TAPa tag to the CSN3 subunit (CSN3-TAPa). Molecular and functional characterization of the CSN3-TAPa was carried out prior to purification using the TAPa system. The capacity of the CSN3-TAPa fusion to complement the lethal *csn3* phenotype was assessed using plants containing a T-DNA insertion in the *CSN3* locus (Figure 3a) (Alonso *et al.*, 2003). *CSN3-TAPa*-containing transgenic plants in the mutant background (*CSN3-TAPa*

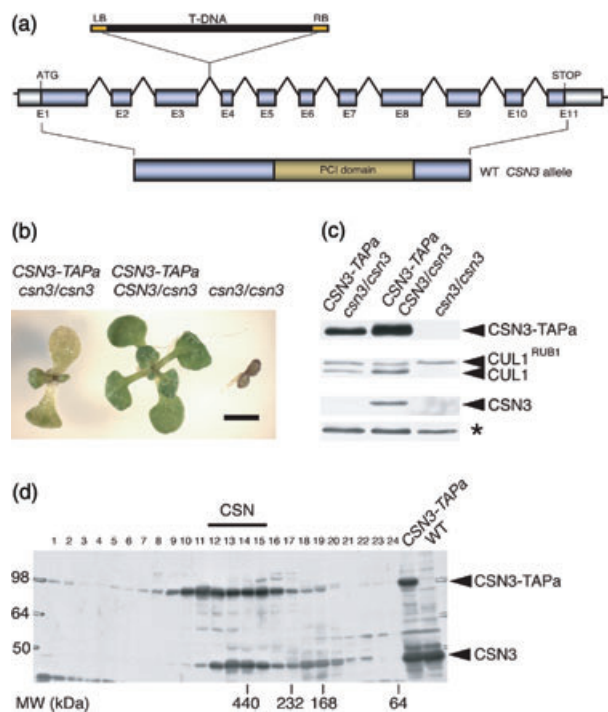


Figure 3. CSN3-TAPa functional and molecular properties.

(a) Diagrammatic representation of the T-DNA insertion in the *CSN3* locus. The *CSN3* gene contains 11 exons (E1–11). A T-DNA insertion (Salk_000593) within the third intron of the *CSN3* gene produces a null *csn3* mutant allele (*csn3-1*). The PCI (Proteasome, COP9 signalosome, Initiation factor 3) domain for CSN3 is shown.

(b) *csn3* mutant complementation analysis. Seedlings were grown for 12 days under continuous white light conditions ($110 \mu\text{mol m}^{-2} \text{sec}^{-1}$) before the picture was taken. Scale bar, 0.2 cm.

(c) CSN3-TAPa-containing CSN complex derubylation of CUL1. Seedlings were grown as described in Figure 3(b). Immunoblots were performed using α -myc, α -CUL1 and α -CSN3 antibodies (from top to bottom). An asterisk indicates a non-specific band used as loading control.

(d) CSN3-TAPa incorporation into the CSN complex. Gel filtration profile fractions of protein extract from 12-day-old seedlings expressing CSN3-TAPa in a heterozygous *csn3* mutant background (*CSN3-TAPa*) were subjected to immunoblot analysis using the α -CSN3 antibody. Wild type (WT) plant protein extract was used as a control. The positions of the molecular weight standards are labeled at the bottom. The fraction numbers containing the endogenous COP9 signalosome are indicated (CSN).

csn3/csn3 overcame the *csn3* lethal phenotype, although their development was delayed when compared with transgenic plants in a heterozygous mutant background (*CSN3-TAPa CSN3/csn3*) (Figure 3b). This result suggests that the CSN3-TAPa fusion largely retains wild type CSN3 functionality. The CSN3-TAPa functionality was independently assessed by testing the ability of the CSN3-TAPa-containing CSN to derubylate cullin 1 (CUL1) *in vivo* (Figure 3c). Extracts from *CSN3-TAPa csn3/csn3* lines contained both rubylated and unmodified CUL1, similar to that observed in extracts from *CSN3-TAPa CSN3/csn3* lines and to that shown in wild-type plants (Schwechheimer *et al.*, 2001). In contrast, extracts from *csn3* mutant plants (*csn3/csn3*) contained only rubylated CUL1 (Figure 3c).

Gel filtration assays were performed to confirm incorporation of CSN3-TAPa into the CSN complex (Figure 3d). A Superose 6 column was used in the gel filtration analysis of proteins extracts from *CSN3-TAPa CSN3/csn3* plants. After immunoblotting against CSN3, we observed similar protein levels and band profile for CSN3-TAPa as with endogenous CSN3. The size difference between the peak fractions of CSN3-TAPa and endogenous CSN3 may be due to the presence of the TAPa tag. As CSN3-TAPa protein accumulated in bigger fractions than those corresponding to its expected size (92 kDa) it is likely that all of the CSN3-TAPa was incorporated in the CSN complex and other possible CSN3-containing complexes.

CSN3-TAPa alternative tandem affinity purification

CSN3-TAPa plants were used in TAPa purification assays along with plants harboring an N-terminal fusion of the TAPa tag to GFP (TAPa-GFP) which was used as a negative control. Protein extracts were incubated with IgG-coated beads and then treated with 3C protease. In preliminary studies, we observed a more efficient TAPa-tagged protein recovery using metal affinity chromatography than using myc epitope immunoprecipitation (data not shown). Therefore, the second affinity purification step was performed by incubating the 3C-digested eluates with nickel (Ni)-coated resin and elution was performed using imidazole-containing buffer. In order to determine the recovery of TAPa-tagged protein after each purification step, protein extracts, flow through fractions and eluates were subjected to immunoblot analysis using an α -myc antibody (Figure 4a). Both TAPa-GFP and CSN3-TAPa proteins showed a highly efficient binding to IgG beads but adsorption to Ni beads was slightly better for TAPa-GFP protein. TAPa-tagged protein recovery from IgG and Ni beads appeared to be very efficient for both TAPa fusions.

To examine the feasibility of our system to co-purify TAPa fusion-associated proteins in the same complex, protein samples, isolated as described above, were separated by SDS-PAGE and visualized by silver staining (Figure 4b, right). In addition to the band corresponding to the TAPa fusion, several specific bands were observed in the CSN3-TAPa lane. Immunoblot analysis using antibodies raised against different CSN subunits demonstrated that these specific bands correspond to members of the CSN complex (Figure 4b, left). There were very little contaminating proteins in both TAPa-GFP and CSN3-TAPa samples except the proteins added during the purification procedure (the IgG heavy and light chains and the 3C protease). Finally, a specific band was observed that co-purified with the TAPa-GFP fusion. This band appeared to be a degradation product of the TAPa-GFP protein as a band of a similar size was detected in the immunoblots against the myc epitope (Figure 4a).

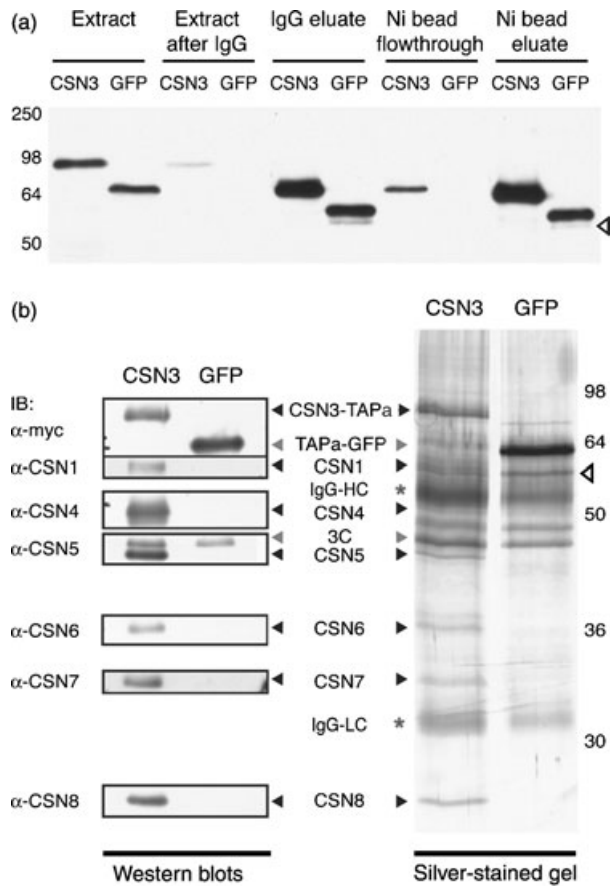


Figure 4. CSN3-TAPa alternative tandem affinity purification.

(a) Immunoblot of different fractions obtained during the CSN3-TAPa purification. Protein extracts from *CSN3-TAPa* (CSN3) and *TAPa-GFP* (GFP, negative control) plants were subjected to TAPa purification. Proteins corresponding to each fraction obtained were separated on a 12% SDS-PAGE gel. The α -myc antibody was used for immunoblotting. An empty arrowhead points to a truncated version of the TAPa-GFP protein. The following fractions are shown: Protein extract (extract, 0.1%), unbound protein after IgG bead incubation (extract after IgG, 0.1%), eluate from IgG beads using 3C protease (IgG eluate, 1%), discarded Ni-NTA column flow through fraction (Ni beads flow through, 1%) and final purified protein (Ni beads eluate, 4%). Percentages indicate the amount of protein loaded relative to the total amount of protein in each sample.

(b) The COP9 signalosome protein band visualization in purified CSN3-TAPa samples. CSN3-TAPa (CSN3) and TAPa-GFP (GFP) proteins were purified using the TAPa procedure and separated on a 12% SDS-PAGE gel. Immunoblotting using antibodies listed in the left panel was performed to recognize six of seven other COP9 signalosome subunits tested. Black arrowheads indicate the position of each subunit protein band, both in the immunoblots and in the silver-stained gel (right panel). The position of the TAPa-GFP and the 3C proteins is shown with gray arrowheads. Asterisks indicate the position of the IgG heavy and light chains (IgG-HC and IgG-LC, respectively). An empty arrowhead points to a truncated version of the TAPa-GFP protein. For immunoblotting and silver staining, 2 and 10%, respectively, of the Ni bead eluates were used.

Mass spectrometry identification of TAPa-purified CSN subunits

To demonstrate the suitability of TAPa-purified proteins for mass spectrometry identification, a large-scale TAPa purification was carried out using a total of 90 g *CSN3-TAPa*

CSN1

MERDEEASGPMEMCTNGGEETSNNRPIISGEPLDI
EAYAALYKGRTKIMRLLFIANHCGGNHALQFDALRM
AYDEIKK**KGENTQLFR**EVVNKIGNRLGEKYGMDLAWC
EAVDRRAEQKVK**LENELSSYR**TNLIKESIRMGYND
FGDFYYACGMLGDAFNKYIRTRDYCTTTKHI IHMCM
NAILVSIEMGQFTHVTSYVNK**AEQNPETLEPMVNAK**
LRCASGLAHLELKKYKLAARKFLDVNPELGNSYNEV
IAPQDIATYGGICALASFDRSELKQK**VIDNINFRNF**
LELVDPVRLELINDFYSSR**YASCLEYLASLKSNNLLD**
IHLHDHVDTLYDQIRKKALIQYTLFPVSVDLSRMAD
AFKTSVSGLEK**ELEALITDNOIQAR**IDSHNKILYAR
HADQRNATFQK**VLQMGNEFDR**DVRAMLLRANLLKHE
YHARSARKL

CSN8

MDLSPVKEALAAKSFDKIADICDTLMLQVASEGIEY
HDDWPYAIHLLGYFYVDDCDSARFLWKRIPTAIKER
KPEVVAAWGIGQKLWTHDYAGVYEAIR**GYDWSQEAK**
DMVAAFSDLYTKRMFQLLSAYSTITIHDLALFLGM
TEDDATTYVVENGWTVDAASQMASVKKQAVKREQKV
DSSKLQR**LTEYVFHLEH**

Figure 5. CSN1 and CSN8 identification by mass spectrometry analysis.

Amino acid sequences in boxes correspond to Arabidopsis CSN1 or CSN8 peptides identified by MS/MS mass spectrometry analysis of TAPa-purified protein samples.

plant material. In TAP purification of yeast protein complexes, it is recommended that independent purifications in parallel be performed, instead of a single large TAP purification if the purification has to be scaled up (Puig *et al.*, 2001). Previous experiments performed in our laboratory using the TAPa purification procedure agreed with this recommendation (data not shown). Therefore, scaling up was carried out by processing six independent *CSN3-TAPa* samples in parallel. Ni bead eluates were pooled, and proteins were separated by SDS-PAGE. Protein bands were visualized by Coomassie brilliant blue staining (data not shown). Bands corresponding to CSN1 and CSN8, as identified by Western blot analysis, were excised and subjected to mass spectrometry analysis to further confirm their identity. As a result, eight and four peptides were obtained with a 100% match to Arabidopsis CSN1 and CSN8 proteins, respectively (Figure 5). Therefore, we conclude that the TAPa purification enables protein enrichment at levels and quality suitable for mass spectrometry analysis.

A large-scale suitability assessment of Arabidopsis TAPa system

In addition to *CSN3*, 30 genes involved in the light signaling pathway and/or in the ubiquitin-26S proteasome pathway

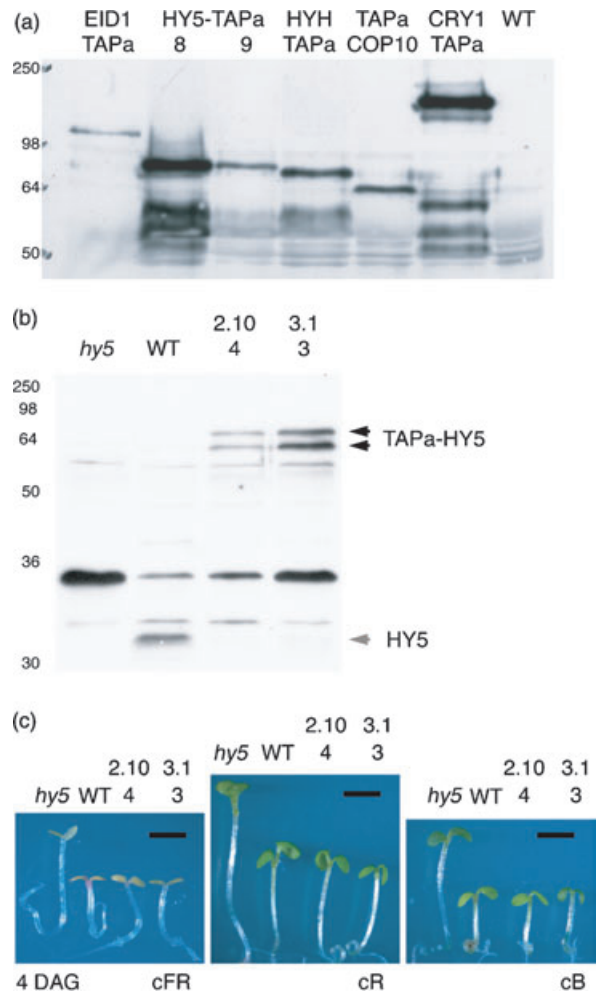
Table 1 Summary of transgenic lines expressing TAPa fusions

Gene	C-TAPa fusion		N-TAPa fusion	
	Transgenic line stage	Fusion expression	Transgenic line stage	Fusion expression
<i>CRY1</i>	T ₂	Yes	T ₃	Yes
<i>CRY2</i>	T ₂	Yes	T ₂	n.a.
<i>PHYA</i>	T ₂	Yes	T ₂	n.a.
<i>PHYB</i>	T ₄	Yes	–	–
<i>FHY1</i>	T ₂	No	T ₂	No
<i>FAR1</i>	T ₂	n.a.	T ₂	n.a.
<i>FHY3</i>	T ₂	n.a.	T ₂	n.a.
<i>FIN219</i>	–	–	T ₂	n.a.
<i>LAF1</i>	T ₂	No	–	–
<i>PAT1</i>	T ₂	n.a.	–	–
<i>SPA1</i>	–	–	T ₄	Yes
<i>EID1</i>	T ₃	Yes	–	–
<i>COI1</i>	T ₂	Yes	T ₂	Yes
<i>UFO</i>	T ₄	Yes	T ₄	Yes
<i>ASK1</i>	T ₂	Yes	T ₂	Yes
<i>AtCUL1</i>	T ₂	Yes	T ₄	Yes
<i>AtCUL3</i>	T ₃	Yes	T ₃	Yes
<i>RBX1</i>	T ₂	Yes	T ₄	Yes
<i>CIP8</i>	T ₂	Yes	–	–
<i>COP1</i>	T ₂	No	T ₂	Yes
<i>COP10</i>	T ₂	Yes	T ₃	Yes
<i>DET1</i>	–	–	T ₂	Yes
<i>CSN1</i>	–	–	T ₂	Yes
<i>CSN3</i>	T ₃	Yes	T ₂	No
<i>CSN4</i>	T ₄	Yes	T ₂	Yes
<i>CSN5</i>	T ₂	Yes	T ₂	Yes
<i>CSN8</i>	T ₂	Yes	T ₂	Yes
<i>HFR1</i>	T ₂	No	T ₂	No
<i>HY5</i>	T ₂	Yes	T ₄	Yes
<i>HYH</i>	T ₂	Yes	T ₂	Yes
<i>PIF3</i>	T ₂	n.a.	T ₂	n.a.
<i>smGFP4</i>	–	–	T ₃	Yes

The transgenic line stage represents the last generation in which fusion expression was analyzed. The expression status for the TAPa fusions is shown as: yes, expression detectable in immunoblots; no, not detectable; n.a., data not available; –, transgenic line not generated.

were also cloned into our TAPa vectors. The list of cloned genes includes members of the CSN complex, SCF type- and RING type-E3 ligases components, photoreceptors and several other positive and negative regulators of photomorphogenesis (for a complete list see Table 1). Although the majority of the genes, 21, were cloned into both N-terminal and C-terminal TAPa vectors, for nine genes just one kind of fusion was performed.

Independent Arabidopsis transgenic lines for each TAPa fusion were obtained and the corresponding fusion protein levels in transgenic plants for 43 constructs (including TAPa fusions to *CSN3*) were analyzed using immunoblots against the myc epitope. We observed TAPa fusion expression in transgenic lines for 36 of 43 constructs analyzed (Table 1). In most cases, expression appeared to be independent of the fusion orientation. However, in two specific cases (*CSN3* and

**Figure 6.** TAPa transgenic line characterization.

(a) Protein expression levels for several typical TAPa fusions. Total protein samples (40 µg) extracted from independent transgenic lines grown for 12 days in continuous white light were loaded onto a 12% SDS-PAGE gel. Immunoblotting was performed using an α -myc antibody.

(b) TAPa-HY5 protein expression. Seedlings corresponding to the *hy5-215* mutant background (*hy5*), Columbia wild type (WT), and two independent transgenic lines harboring a *TAPa-HY5* transgene (2.10.4 and 3.1.3) were grown for 4 days in continuous far red light (125 µmol m⁻² sec⁻¹). Total protein samples were extracted from them and loaded (40 µg) into a 15% SDS-PAGE gel. Immunoblotting was performed using an α -HY5 antibody. Two black arrowheads show the position of the TAPa-HY5 band doublet. A gray arrowhead points to the endogenous HY5 band.

(c) *hy5* mutant complementation analysis. Seedlings corresponding to the *hy5-215* mutant background (*hy5*), Columbia wild type (WT), and two independent transgenic lines harboring a *TAPa-HY5* transgene (2.10.4 and 3.1.3) were grown for 4 days in continuous far red light (125 µmol m⁻² sec⁻¹, cFR), continuous red light (200 µmol m⁻² sec⁻¹, cR) or continuous blue light (5 µmol m⁻² sec⁻¹, cB). Scale bar, 0.2 cm.

COP1) one orientation (C-terminal and N-terminal, respectively) was expressed while the other orientation was not. Fusion expression levels varied greatly among transgenic lines for different genes, even when protein extracts were obtained from plants grown in the same conditions (Figure 6a). Similar variation was observed among independent

transgenic lines for the same TAPa fusion possibly reflecting positional effects at the transcriptional level due to transgene location (Figure 6a,b). Fusion expression band patterns showed, in most cases, one major band corresponding to the expected TAPa-tagged protein size. However, in some transgenic lines, such as *HY5* and *HYH TAPa*-containing lines, the fusion size was much bigger than expected. This abnormal electrophoretic behavior seems to be independent of the TAPa tag as it is inherent to those target proteins (Holm *et al.*, 2002; Osterlund *et al.*, 2000). In some cases, in addition to the major band, we observed other specific minor bands, probably corresponding to truncated versions of the corresponding TAPa fusion. The presence of a doublet was observed in the N-terminal TAPa-tagged *HY5* fusion (TAPa-*HY5*) even when protein samples were denatured with urea prior to SDS-PAGE (Figure 6b). So far, a possible post-translational modification of the TAPa-*HY5* fusion which could explain such a pattern has not been identified (data not shown).

Functional characterization was performed in several transgenic lines using a mutant phenotype complementation analysis (Table 2). Transgenic plants were grown in the specific conditions reported for each genetic background and different parameters were analyzed and compared with those in mutant and wild-type plants grown in the same conditions (see Experimental procedures). In the case of TAPa-*SPA1*, its ability to complement the mutant phenotype has been previously reported (Saijo *et al.*, 2003). *CRY2*-TAPa fusions also completely rescued the photomorphogenic defects in the *cry2* mutant when grown under blue light conditions. However, both *PHYA*- and *HYH*-TAPa fusions failed to complement their corresponding mutant phenotypes under the growth conditions tested. Partial complementation events were also observed as exemplified by the *CSN3*-TAPa lines. Further examples include the TAPa fusions to *HY5* or *COP1* which only partially rescued their respective mutant phenotypes. The

degree of complementation also varied among different proteins and growth conditions. For example, independent N-terminal TAPa-*HY5* transgenic lines fully complemented the mutant background when grown under continuous red (cR) or blue (cB) light. However, the same transgenic lines grown under continuous far red (cFR) light showed a partial complementation (Figure 6c).

Taken together, these results suggest that, even if over-expressing transgenic lines are used, the TAPa-tagged protein expression level, band pattern and function depend largely on the nature of the protein of interest and the regulatory mechanisms controlling the endogenous protein levels and function.

Discussion

The feasibility of TAP approaches to allow epitope tagging and affinity purification of a large number of protein complexes from yeast cells has been already shown (Gavin *et al.*, 2002; Graumann *et al.*, 2004; Puig *et al.*, 2001; Shevchenko *et al.*, 2002). In contrast, application of TAP in plants is just emerging. A general TAP procedure has been described for plants (Rohila *et al.*, 2004), nevertheless, the use of this system applied to endogenous protein complexes purification from stably transformed plants has not been demonstrated. In this study, we describe the use of a TAPa system to isolate multiple subunit protein complexes from stable transgenic plants. The modifications in our TAPa tag and strategy were designed to allow efficient protein purification to be performed at 4°C and to avoid the involvement of strong cation-chelating agents such as EDTA or EGTA used in the original TAP method. These modifications should help to stabilize protein complex structure and activity. In addition, our system offers two different affinity tags, 6xHis and 9xmyc, for the second affinity purification step (Figure 1). The use of His and myc tags provides an alternative purification strategy in case a fusion protein fails to be purified using one of them. The presence of three different tags (2xIgG-BD, 6xHis and 9xmyc) in our TAPa system could allow a triple affinity purification procedure, although this has yet to be demonstrated. All our transgenes are driven by a constitutive promoter which should lead to overexpression of our TAPa fusions. Such overexpression should increase tagged protein incorporation into its corresponding protein complex in those cases in which our protein of interest is the limiting factor for complex formation. Additionally, in case a mutant or suppressed line for a specific gene is not available, overexpression of the tagged protein should help tagged protein incorporation into the protein complex in preference to the endogenous protein.

Molecular characterization of a *CSN3*-TAPa transgenic line demonstrated TAPa-tagged protein incorporation into the CSN complex (Figure 3d). In addition, functional properties inherent to the wild-type *CSN3* were found in the

Table 2 Summary of transgenic lines in which a complementation analysis was carried out

Gene	Mutant background	C-TAPa fusion	N-TAPa fusion
<i>CRY2</i>	<i>cry2-1</i>	Yes	n.a.
<i>PHYA</i>	<i>phyA-301</i>	No	No
<i>SPA1</i>	<i>spa1-3</i>	-	Yes
<i>COP1</i>	<i>cop1-6</i>	No	Partial
<i>CSN3</i>	<i>csn3-1</i>	Partial	n.a.
<i>HY5</i>	<i>hy5-215</i>	Partial	Partial
<i>HYH</i>	<i>hyh</i>	No	n.a.

Complementation results are expressed as: yes, the transgene fully complements the corresponding mutant phenotype; partial, mutant defects, although less severe, are still evident; no, the transgenic line essentially resembles the corresponding mutant line; n.a., data not available; -, transgenic line not generated.

CSN3-TAPa fusion. Thus, the CSN3-TAPa fusion rescued the *csn3* mutant lethal phenotype (Figure 3b) and, moreover, the CSN3-TAPa-containing complex showed CSN-dependent derubylation of cullin 1 *in vivo* (Figure 3c).

Application of the TAPa procedure using a *CSN3-TAPa* expressing transgenic line allowed us to purify the CSN complex (Figure 4). Use of a negative control is recommendable as some proteins appeared as common bands in both TAPa-GFP and CSN3-TAPa-purified samples (Figure 4b). These bands correspond to proteins from the reagents employed (i.e. 3C protease and IgG) and to non-specific interactors to the TAPa tag or to the beads used during purification. In the first case, incubation of beads with acid solution can help to decrease the amount of free IgG in the IgG-coated resin (data not shown). Reduction of the 3C amount can be carried out using glutathione sepharose as 3C protease is commercially available as a fusion to the GST tag. In the case of non-specific interactors, increasing the stringency of the procedure, by using higher concentrations of salt and detergent in the buffer solutions, should help to reduce their level. Purification of CSN was performed under native conditions and the use of crosslinking was avoided. Nevertheless, it could help to stabilize weak interactions leading to an increase in the purification yield and purified protein number (Rohila *et al.*, 2004).

Finally, we intended to assess the feasibility of the TAPa system to be extrapolated to a larger number of genes in Arabidopsis. Using our TAPa tag we generated Arabidopsis transgenic lines for 53 distinct constructs harboring N-terminal or C-terminal TAPa fusions to 31 genes involved in either the ubiquitin/26S proteasome proteolytic regulatory machinery or the photomorphogenesis regulatory pathway (Table 1). Transgenic lines containing an N-terminal TAPa fusion to the *GFP* gene were also obtained. Fusion expression analysis of our transgenic lines showed that transgenic plants from 36 of 43 (83%) constructs analyzed expressed their corresponding fusion proteins (Table 1). Furthermore, we obtained transgenic lines that expressed N-terminal and/or C-terminal fusion constructs for 23 of 26 (88%) genes analyzed. However, in some cases where fusion expression was not observed, we cannot exclude the possibility that optimal growth conditions, starting plant material or experimental conditions were not used.

Large variation in TAPa transgene expression *in planta* between different fusion constructs was observed (Figure 6a). In many cases the presence of truncated proteins in addition to the full-length version as well as fusion proteins larger than the expected size were observed. In the first case, truncated TAPa fusions correlated with a high level of transgene expression, suggesting that the higher the expression is, the more likely the TAPa fusions are processed by non-specific proteases. In the case of unexpected fusion sizes, this particular feature seems to be independent of the TAPa tag as also observed in endogenous

proteins (i.e. HY5 and HYH, Holm *et al.*, 2002; Osterlund *et al.*, 2000).

The presence of a doublet in a specific protein band pattern could reveal the existence of two isoforms for that particular protein. A source for such variation can be post-translational modification. In a previous study using the TAPa tag, it was observed that conjugation of RUB1 occurred on N-terminal TAPa-tagged cullin 1 (TAPa-CUL1). Interestingly, such modification did not occur on C-terminal TAPa-tagged cullin 1 (CUL1-TAPa) revealing that both TAPa fusions have different functional properties. The different properties of these two fusion proteins provided an ideal system for testing their differential association with CAND1 *in vivo* (Feng *et al.*, 2004). In the case of N-terminal TAPa-tagged HY5 fusion (TAPa-HY5) the presence of a doublet was also observed (Figure 6b). It is known that HY5 undergoes phosphorylation and ubiquitination processes *in vivo* (Hardtke *et al.*, 2000; Saijo *et al.*, 2003). However, due to the difference in band size (more than 5 kDa) in the TAPa-HY5 doublet it is unlikely the upper band corresponds to mono-phosphorylated fusion. Immunoblots against ubiquitin ruled out the possibility that an ubiquitinated TAPa-HY5 isoform is part of the observed doublet (data not shown).

Mutant complementation analysis showed that several N-terminal and C-terminal TAPa fusions retained function to that of wild-type proteins (Table 2). The extent of function retention depended on each tagged protein. It could be argued that the big size (33 kDa) of the TAPa tag can affect fusion structure and functionality. However, proteins fused to a smaller version (18 kDa) of the TAPa tag lacking the 9xmyc domain showed a similar degree of complementation as their TAPa counterparts (data not shown). Taken together, these results demonstrate that the TAPa system allows overexpression of functional TAPa-tagged proteins. The tagged protein expression level and functionality degree depend largely on the structural and regulatory features of each protein of study.

In summary, the data presented here demonstrate that the TAPa system allows multi-protein complex isolation from stably transformed plant material. Our TAPa system represents an efficient alternative to other affinity purification systems and classical biochemical protein purification procedures. Protein complex samples obtained by using our TAPa strategy are suitable for mass spectrometry analysis purposes. Application of the TAPa system to high-throughput approaches can be facilitated by easy cloning in the TAPa vectors using their GATEWAY-based sequences. Both transiently and stably transformed *Nicotiana benthamiana* plants expressing C-TAPa fusions have already been obtained (data not shown), thus, demonstrating that the high fusion expression levels found in Arabidopsis TAPa transgenic lines and the suitability of the TAPa procedure can be extended to other plant species or expression systems.

Experimental procedures

TAPa construct generation

The pC-TAPa plasmid was made as follows. The pYL44 plasmid (Liu *et al.*, 2002) was digested with *Hind*III and *Eco*RI and a DNA fragment containing a duplicated CaMV 35S promoter (2×35S) and a Nos terminator (Nos ter) was recovered and cloned into the pZP222 plasmid (Hajdukiewicz *et al.*, 1994) to generate the pYL400 plasmid. The pYL434 was obtained by replacing the 3xflag DNA fragment of pYTV (Gong *et al.*, 2004) with a *Hind*III/*Avr*II-digested PCR product containing nine repeats of the myc epitope (9xmyc). A PCR product containing a TMV U1 Ω sequence, a GATEWAY cloning cassette (*att*R1::Cm^R::*ccdB*::*att*R2; GATEWAY, Invitrogen), a six His repeat (6xHis), the 9xmyc, a 3C protease cleavage site and two copies of the IgG binding domain (2xIgG-BD) was obtained using pYL434 as a template and the following primers; OYL646, 5'-ccggctagagatattttacaacaattaccaacaacaacaacaacaacaacattacaattcattttacaattacaagttgtacaaaaaagctga-3' and OYL647, 5'-gggttacctc-gagagctcctctaggatcagcgggtttgggtca-3'. This PCR product was digested using *Stu*I and *Kpn*I and cloned into the pYL400 plasmid to generate the pC-TAPa construct (also named as pYL436, pPTV and pYL TAP Ct). Sequence analysis of each DNA fragment cloned was performed after every cloning step.

The pN-TAPa plasmid was made as follows. PCR products were obtained using the pC-TAPa plasmid as a template and cloned successively into the pBluescript SK+ phagemid in the following order. The DNA fragment corresponding to the 2 × 35S::TMV U1 Ω sequence was amplified using the primers 5'-agttggatcc-gccagggtttccagtcacg-3' and 5'-tttgatcgatcttgtaattgtaaatagtaattg-taatg-3' and cloned using *Bam*HI and *Cl*al. The DNA fragment corresponding to the 2xIgG-BD-3C sequence was amplified using the primers 5'-gagctatcgatggccaccatggcgcaacacagaagaagccgtag-3' and 5'-tttgtaattcgggcccctggaacagaactccagctaccgagctcaaatccgctc-tac-3' and cloned using *Cl*al and *Eco*RI. The DNA fragment corresponding to the 6xHis-9xmyc sequence was amplified using the primers 5'-aaaagaattccatcaccatcaccatcacgcccgtcctagaactagtgg-3' and 5'-ttttctcagagcccggggatccactagtgg-3' and cloned using *Eco*RI and *Xho*I. A DNA fragment corresponding to the *att*R1::Cm^R::*ccdB*::*att*R2 sequence was amplified using the primers 5'-tattctcagagaacaagttgtacaaaaaagctgaacg-3' and 5'-ttttgtacct-taaaccacttgtaacaagaagctg-3' and cloned using *Xho*I and *Kpn*I. The whole N-TAPa expression cassette was obtained by digesting with *Hind*III and *Kpn*I and cloning into the pYL400 plasmid to obtain the pN-TAPa construct (previously named as pYL TAP Nt). Sequence analysis of each DNA fragment cloned was performed after every cloning step. The pN-TAPa cloning site is not in-frame with the two lysine codons (AAA-AAA) in the upstream *att*R1 sequence; it is 2 bp misplaced (CAA-AAA-AGC).

Prior to cloning into the pC-TAPa and pN-TAPa plasmids, the genes analyzed in this study were PCR-amplified using *att*B sequence containing primers and cloned into the pDONR 201 plasmid using the BP reaction (GATEWAY; Invitrogen). At this stage, DNA sequence analysis was performed. The transfer of genes from the pDONR 201 plasmid to the corresponding TAPa vector was performed using LR reaction (GATEWAY; Invitrogen).

Plant material, growth conditions and complementation analysis

Arabidopsis thaliana plants used in this study were of the Columbia-0 ecotype unless otherwise stated. The *cry2-1* (Ahmad *et al.*, 1998), *phyA-301* (Fry *et al.*, 2002), *spa1-3* (RLD ecotype; Hoecker *et al.*,

1999), *cop1-6* (McNellis *et al.*, 1994), *hy5-215* (Ang and Deng, 1994) and *hyh* (Wassilewskija ecotype; Holm *et al.*, 2002) mutants have been previously described. The *csn3-1* mutant described in this study corresponds to a T-DNA insertion line from the Salk collection (Salk_000593, Alonso *et al.*, 2003). Seeds were surface-sterilized, placed on MS plates (Gibco, Cleveland, OH, USA) containing 0.3% sucrose and cold-treated for 3 days. Vernalized seeds were exposed to white light for 12 h and then transferred to continuous light conditions. Depending on each transgenic line, different light conditions were used to check mutant complementation: *CRY2*, *HY5* and *HYH* TAPa lines were grown for 4 days in cB light (5 μ mol m⁻² sec⁻¹). *PHYA* and *HY5* TAPa lines were grown for 4 days in cFR light (125 μ mol m⁻² sec⁻¹). *HY5* TAPa lines were grown for 4 days in cR light (200 μ mol m⁻² sec⁻¹); TAPa-COP1 lines were grown for 4 days in continuous darkness. *CSN3-TAPa* lines were grown for 12 days in continuous white light (110 μ mol m⁻² sec⁻¹). To obtain adult plants, 7–9-day-old light-grown seedlings were transferred to soil and grown in standard long day (16 h light/8 h dark) growth room. All TAPa constructs were transformed into plants by the floral dip method (Clough and Bent, 1998). *Agrobacterium tumefaciens* strains GV3101 and C58C1 were used in the transformation process. Hypocotyl length of plants, grown as described above, was measured in order to perform the mutant complementation analysis. In the case of cFR light-grown TAPa-HY5 plants, anthocyanin concentration was analyzed as previously described (McNellis *et al.*, 1994).

Western blot analysis and gel filtration chromatography

Arabidopsis tissues were homogenized in an extraction buffer containing 50 mM Tris-HCl pH 7.5, 150 mM NaCl, 10% glycerol, 0.1% Nonidet P-40, 1 mM DTT, 1 mM PMSF, and 1x complete protease inhibitor cocktail (Roche, Indianapolis, IN, USA). Protein extracts were centrifuged twice at 4°C for 10 min each, and protein concentration in the supernatant determined by Bradford assay (Bio-Rad, Hercules, CA, USA). Protein samples were boiled in sample buffer, run on SDS-PAGE gels (7.5, 10, 12, or 17.5%) and blotted onto polyvinylidene difluoride (PVDF) membranes (Millipore, Bedford, MA, USA). The blots were probed with different primary antibodies. To confirm the presence of a fusion doublet in TAPa-HY5 lines, protein extracts were boiled in 8 M urea sample buffer prior to SDS-PAGE.

For gel filtration assays, protein extract (200 μ g) from *CSN3-TAPa* seedlings in a heterozygous *csn3* mutant background was injected on a Superose 6 column (Amersham Biosciences, Piscataway, NJ, USA). Twenty-four fractions of 0.5 ml were collected. Proteins on each fraction were concentrated using STRATARESIN (Stratagene, La Jolla, CA, USA), run on 10% SDS-PAGE gel and blotted using the α -CNS3 antibody (Peng *et al.*, 2001a).

Other primary antibodies used in this study include α -myc monoclonal antibody (Saijo *et al.*, 2003), α -CUL1 (Wang *et al.*, 2003), α -HY5 (Osterlund *et al.*, 2000), α -CSN1 (Staub *et al.*, 1996), α -CSN4 (Serino *et al.*, 1999), α -CSN5 (Kwok *et al.*, 1998), α -CSN6 (Peng *et al.*, 2001b), α -CSN7 (Karniol *et al.*, 1999), and α -CSN8 (Chamovitz *et al.*, 1996).

TAPa purification procedure

CSN3-TAPa and TAPa-GFP seedlings (15 g, fresh weight) grown in complete media for 18 days under continuous white light conditions were ground in liquid nitrogen, thawed in 2 volumes of extraction buffer (50 mM Tris-HCl pH 7.5, 150 mM NaCl, 10% glycerol, 0.1% Nonidet P-40, 1 mM PMSF, and 1x complete protease

inhibitor cocktail; Roche), filtered through four layers of cheese-cloth, and centrifuged at 12 000 *g* for 10 min at 4°C. The protein concentration in the supernatant was determined by Bradford assay (Bio-Rad). Extracts containing similar amounts of total protein were incubated with 500 µl IgG beads (Amersham Biosciences) for 2 h at 4°C with gentle rotation. After centrifugation at 150 *g* for 3 min at 4°C, the IgG beads were recovered and washed three times with 10 ml of washing buffer (50 mM Tris-HCl pH 7.5, 150 mM NaCl, 10% glycerol, 0.1% Nonidet P-40) and once with 10 ml of cleavage buffer (50 mM Tris-HCl pH 7.5, 150 mM NaCl, 10% glycerol, 0.1% Nonidet P-40, 1 mM DTT). Elution from the IgG beads was performed by incubation with 50 µl (100 units) of 3C protease (Prestige protease; Amersham Biosciences) in 5 ml of cleavage buffer at 4°C with gentle rotation. Supernatants were recovered after centrifugation at 150 *g* for 3 min at 4°C and stored. The IgG beads were washed with 5 ml of washing buffer and centrifuged again. Supernatants were recovered and the eluates pooled. Pooled eluates were loaded into 1 ml of Ni-NTA resin (Qiagen, Valencia, CA, USA) packed into a 10-ml disposable polypropylene chromatography column (Bio-Rad). Flow throughs were loaded again into the Ni-NTA column. After washing the column with 30 ml of washing buffer, elution was performed using 5 ml of imidazole containing buffer (50 mM Tris-HCl pH 7.5, 150 mM NaCl, 10% glycerol, 0.1% Nonidet P-40, 0.05 M imidazole). All the steps in the purification procedure were carried out at 4°C. Proteins in each fraction (except total plant extracts) were concentrated using STRATARESIN (Stratagene) and separated on a 12% SDS-PAGE gel. Protein bands were visualized, independently, by immunoblotting using the α -myc antibody and by silver staining.

For large-scale TAPa purification, six *CSN3-TAPa* plant samples (15 g, fresh weight each) were processed in parallel as described above. Final eluates were pooled, proteins were precipitated using STRATARESIN and separated on a 12% SDS-PAGE gel. Protein bands were visualized by Coomassie brilliant blue staining.

Mass spectrometry analysis

TAPa-purified protein bands corresponding to CSN1 and CSN8 were excised from SDS-PAGE gel and subjected to mass spectrometry analysis as described below. The protein bands were cut in small pieces and washed successively at room temperature with 250 µl 50% H₂O/50% CH₃CN for 5 min, with 250 µl 50% CH₃CN/50 mM NH₄HCO₃ for 30 min and with 250 µl 50% CH₃CN/10 mM NH₄HCO₃ for 30 min. Gel pieces were completely dried using a SpeedVac. Trypsin digestion was performed by incubation of samples with 0.1 µg modified trypsin (Promega, Madison, WI, USA) per 15 mm³ of gel in 15 µl 10 mM NH₄HCO₃ for 24 h at 37°C. Samples were dissolved in 60 µl 0.05% TFA, 5% CH₃CN prior to mass spectrometry analysis. Protein digests were analyzed using LC/MS/MS on a Q-ToF API mass spectrometer (Waters/Micromass, Milford, MA, USA). Ten microliters of sample was directly injected onto a 100 µm × 150 mm Atlantis column running at 500 nl min⁻¹. An 85-min gradient was used in order to obtain good peptide separation. Buffer A consisted of 98% water, 2% CH₃CN, 0.1% acetic acid, and 0.01% TFA. Buffer B contained 80% CH₃CN, 20% water, 0.09% acetic acid, and 0.01% TFA. Data-dependent acquisition was performed so that the mass spectrometer switched automatically from MS to MS/MS modes when the total ion current increased above the 1.5 counts sec⁻¹ threshold set point. In order to obtain good fragmentation, a collision energy ramp was set for the different mass sizes and charge states, giving preference to doubly and triply charged species for fragmentation over singly charged species.

All MS/MS outputs were processed using the MASCOT algorithm (Hirose et al., 1993) for un-interpreted MS/MS spectra after

using the MASCOT Distiller program (Matrix Science Ltd, London, UK) to generate MASCOT compatible files. The MASCOT Distiller program combines sequential MS/MS scans from profile data that have the same precursor ion. Using the MASCOT database search algorithm, proteins were considered as identified when MASCOT listed them as significant and more than two peptides matched the same protein. The database searched was the National Center for Biotechnology Information non-redundant database. The parameters used for searching were as follows: partial methionine oxidation and acrylamide-modified cysteine, a peptide tolerance of ±0.6 Da, MS/MS fragment tolerance of ±0.4 Da, and peptide charges of +2 or +3.

Acknowledgements

We are grateful to J.A. Sullivan for critical reading of the manuscript, to C. Yi, Y. Yanagawa and N. Wei for their advice and stimulating discussions, to T. Tsuge for the monoclonal α -myc antibody and to L. Li for his assistance in the *CSN3-TAPa* line generation. Our work was supported by grants from NIH (GM047850) and NSF 2010 program (MCB-0115870) to X.W.D. and NSF (DBI-0211872) to S.P.D.K. V.R. is supported by a Human Frontiers Science Program long-term fellowship; Y.S. is a Japanese Society for Promotion of Science postdoctoral fellow. Both pN-TAPa and pC-TAPa (deposited as pYL436) vectors are available at the Ohio State University Stock Center.

References

- Ahmad, M., Jarillo, J.A., Smirnova, O. and Cashmore, A.R. (1998) Cryptochrome blue-light photoreceptors of *Arabidopsis* implicated in phototropism. *Nature*, **392**, 720–723.
- Alonso, J.M., Stepanova, A.N., Leisse, T.J. et al. (2003) Genome-wide insertional mutagenesis of *Arabidopsis thaliana*. *Science*, **301**, 653–657.
- Ang, L.H. and Deng, X.W. (1994) Regulatory hierarchy of photomorphogenic loci: allele-specific and light-dependent interaction between the *HY5* and *COP1* loci. *Plant Cell*, **6**, 613–628.
- Chamovitz, D.A., Wei, N., Osterlund, M.T., von Arnim, A.G., Staub, J.M., Matsui, M. and Deng, X.W. (1996) The COP9 complex, a novel multi-subunit nuclear regulator involved in light control of a plant developmental switch. *Cell*, **86**, 115–121.
- Clough, S.J. and Bent, A.F. (1998) Floral dip: a simplified method for *Agrobacterium*-mediated transformation of *Arabidopsis thaliana*. *Plant J.* **16**, 735–743.
- Cope, G.A., Suh, G.S., Aravind, L., Schwarz, S.E., Zipursky, S.L., Koonin, E.V. and Deshaies, R.J. (2002) Role of predicted metalloprotease motif of Jab1/Csn5 in cleavage of Nedd8 from Cul1. *Science*, **298**, 608–611.
- Deng, X.W., Dubiel, W., Wei, N. et al. (2000) Unified nomenclature for the COP9 signalosome and its subunits: an essential regulator of development. *Trends Genet.* **16**, 202–203.
- Feng, S., Shen, Y., Sullivan, J.A., Rubio, V., Xiong, Y., Sun, T.P. and Deng, X.W. (2004) *Arabidopsis* CAND1, an unmodified CUL1-interacting protein, is involved in multiple developmental pathways controlled by ubiquitin/proteasome-mediated protein degradation. *Plant Cell*, **16**, 1870–1882.
- Forler, D., Kocher, T., Rode, M., Gentzel, M., Izaurralde, E. and Wilm, M. (2003) An efficient protein complex purification method for functional proteomics in higher eukaryotes. *Nat. Biotechnol.* **21**, 89–92.
- Fry, R.C., Habashi, J., Okamoto, H. and Deng, X.W. (2002) Characterization of a strong dominant phytochrome A mutation unique

- to phytochrome A signal propagation. *Plant Physiol.* **130**, 457–465.
- Gallie, D.R.** (2002) The 5'-leader of tobacco mosaic virus promotes translation through enhanced recruitment of eIF4F. *Nucleic Acids Res.* **30**, 3401–3411.
- Gavin, A.C., Bosche, M., Krause, R. et al.** (2002) Functional organization of the yeast proteome by systematic analysis of protein complexes. *Nature*, **415**, 141–147.
- Gong, W., Shen, Y.P., Ma, L.G. et al.** (2004) Genome-wide ORFeome cloning and analysis of *Arabidopsis* transcription factor genes. *Plant Physiol.* **135**, 773–782.
- Graumann, J., Dunipace, L.A., Seol, J.H., McDonald, W.H., Yates, III, J.R., Wold, B.J. and Deshaies, R.J.** (2004) Applicability of tandem affinity purification MudPIT to pathway proteomics in yeast. *Mol. Cell Proteomics*, **3**, 226–237.
- Groisman, R., Polanowska, J., Kuraoka, I., Sawada, J., Saijo, M., Drapkin, R., Kisselev, A.F., Tanaka, K. and Nakatani, Y.** (2003) The ubiquitin ligase activity in the DDB2 and CSA complexes is differentially regulated by the COP9 signalosome in response to DNA damage. *Cell*, **113**, 357–367.
- Gully, D., Moinier, D., Loiseau, L. and Bouveret, E.** (2003) New partners of acyl carrier protein detected in *Escherichia coli* by tandem affinity purification. *FEBS Lett.* **548**, 90–96.
- Hajdukiewicz, P., Svab, Z. and Maliga, P.** (1994) The small, versatile pPZP family of *Agrobacterium* binary vectors for plant transformation. *Plant Mol. Biol.* **25**, 989–994.
- Hardtke, C.S., Gohda, K., Osterlund, M.T., Oyama, T., Okada, K. and Deng, X.W.** (2000) HY5 stability and activity in *Arabidopsis* is regulated by phosphorylation in its COP1 binding domain. *EMBO J.* **19**, 4997–5006.
- Hirosawa, M., Hoshida, M., Ishikawa, M. and Toya, T.** (1993) MASCOT: multiple alignment system for protein sequences based on three-way dynamic programming. *Comput. Appl. Biosci.* **9**, 161–167.
- Hoecker, U., Tepperman, J.M. and Quail, P.H.** (1999) SPA1, a WD-repeat protein specific to phytochrome A signal transduction. *Science*, **284**, 496–499.
- Holm, M., Ma, L.G., Qu, L.J. and Deng, X.W.** (2002) Two interacting bZIP proteins are direct targets of COP1-mediated control of light-dependent gene expression in *Arabidopsis*. *Genes Dev.* **16**, 1247–1259.
- Karniol, B., Malec, P. and Chamovitz, D.A.** (1999) *Arabidopsis FUSCA5* encodes a novel phosphoprotein that is a component of the COP9 complex. *Plant Cell*, **11**, 839–848.
- Knuesel, M., Wan, Y., Xiao, Z., Holinger, E., Lowe, N., Wang, W. and Liu, X.** (2003) Identification of novel protein-protein interactions using a versatile mammalian tandem affinity purification expression system. *Mol. Cell Proteomics*, **2**, 1225–1233.
- Kwok, S.F., Solano, R., Tsuge, T., Chamovitz, D.A., Ecker, J.R., Matsui, M. and Deng, X.W.** (1998) *Arabidopsis* homologs of a c-Jun coactivator are present both in monomeric form and in the COP9 complex, and their abundance is differentially affected by the pleiotropic *cop/det/fus* mutations. *Plant Cell*, **10**, 1779–1790.
- Liu, Y., Schiff, M., Marathe, R. and Dinesh-Kumar, S.P.** (2002) Tobacco *Rar1*, *EDS1* and *NPR1/NIM1* like genes are required for N-mediated resistance to tobacco mosaic virus. *Plant J.* **30**, 415–429.
- Lyapina, S., Cope, G., Shevchenko, A., Serino, G., Tsuge, T., Zhou, C., Wolf, D.A., Wei, N., Shevchenko, A. and Deshaies, R.J.** (2001) Promotion of NEDD8-CUL1 conjugate cleavage by COP9 signalosome. *Science*, **292**, 1382–1385.
- McNellis, T.W., von Arnim, A.G. and Deng, X.W.** (1994) Overexpression of *Arabidopsis COP1* results in partial suppression of light-mediated development: evidence for a light-inactivable repressor of photomorphogenesis. *Plant Cell*, **6**, 1391–1400.
- Osterlund, M.T., Hardtke, C.S., Wei, N. and Deng, X.W.** (2000) Targeted destabilization of HY5 during light-regulated development of *Arabidopsis*. *Nature*, **405**, 462–466.
- Peng, Z., Serino, G. and Deng, X.W.** (2001a) A role of *Arabidopsis* COP9 signalosome in multifaceted developmental processes revealed by the characterization of its subunit 3. *Development*, **128**, 4277–4288.
- Peng, Z., Serino, G. and Deng, X.W.** (2001b) Molecular characterization of subunit 6 of the COP9 signalosome and its role in multifaceted developmental processes in *Arabidopsis*. *Plant Cell*, **13**, 2393–2407.
- Puig, O., Caspary, F., Rigaut, G., Rutz, B., Bouveret, E., Bragado-Nilsson, E., Wilm, M. and Seraphin, B.** (2001) The tandem affinity purification (TAP) method: a general procedure of protein complex purification. *Methods*, **24**, 218–229.
- Rigaut, G., Shevchenko, A., Rutz, B., Wilm, M., Mann, M. and Seraphin, B.** (1999) A generic protein purification method for protein complex characterization and proteome exploration. *Nat. Biotechnol.* **17**, 1030–1032.
- Rohila, J.S., Chen, M., Cerny, R. and Fromm, M.E.** (2004) Improved tandem affinity purification tag and methods for isolation of protein heterocomplexes from plants. *Plant J.* **38**, 172–181.
- Saijo, Y., Sullivan, J.A., Wang, H., Yang, J., Shen, Y., Rubio, V., Ma, L., Hoecker, U. and Deng, X.W.** (2003) The COP1-SPA1 interaction defines a critical step in phytochrome A-mediated regulation of HY5 activity. *Genes Dev.* **17**, 2642–2647.
- Schwechheimer, C., Serino, G., Callis, J., Crosby, W.L., Lyapina, S., Deshaies, R.J., Gray, W.M., Estelle, M. and Deng, X.W.** (2001) Interactions of the COP9 signalosome with the E3 ubiquitin ligase SCF^{TIR1} in mediating auxin response. *Science*, **292**, 1379–1382.
- Serino, G. and Deng, X.W.** (2003) The COP9 signalosome: regulating plant development through the control of proteolysis. *Annu. Rev. Plant Biol.* **54**, 165–182.
- Serino, G., Tsuge, T., Kwok, S., Matsui, M., Wei, N. and Deng, X.W.** (1999) *Arabidopsis cop8* and *fus4* mutations define the same gene that encodes subunit 4 of the COP9 signalosome. *Plant Cell*, **11**, 1967–1980.
- Shevchenko, A., Schaft, D., Roguev, A., Pijnappel, W.W., Stewart, A.F. and Shevchenko, A.** (2002) Deciphering protein complexes and protein interaction networks by tandem affinity purification and mass spectrometry: analytical perspective. *Mol. Cell Proteomics*, **1**, 204–212.
- Staub, J.M., Wei, N. and Deng, X.W.** (1996) Evidence for *FUS6* as a component of the nuclear-localized COP9 complex in *Arabidopsis*. *Plant Cell*, **8**, 2047–2056.
- Tomoda, K., Kubota, Y. and Kato, J.** (1999) Degradation of the cyclin-dependent-kinase inhibitor p27^{Kip1} is instigated by Jab1. *Nature*, **398**, 160–165.
- Wang, X., Feng, S., Nakayama, N., Crosby, W.L., Irish, V., Deng, X.W. and Wei, N.** (2003) The COP9 signalosome interacts with SCF^{UFO} and participates in *Arabidopsis* flower development. *Plant Cell*, **15**, 1071–1082.
- Wei, N., Chamovitz, D.A. and Deng, X.W.** (1994) *Arabidopsis* COP9 is a component of a novel signaling complex mediating light control of development. *Cell*, **78**, 117–124.
- Wei, N., Tsuge, T., Serino, G., Dohmae, N., Takio, K., Matsui, M. and Deng, X.W.** (1998) The COP9 complex is conserved between plants and mammals and is related to the 26S proteasome regulatory complex. *Curr. Biol.* **8**, 919–922.

Zhou, C., Seibert, V., Geyer, R., Rhee, E., Lyapina, S., Cope, G., Deshaies, R.J. and Wolf, D.A. (2001) The fission yeast COP9/signalosome is involved in cullin modification by ubiquitin-related Ned8p. *BMC Biochem.* **2**, 7.

Zhou, C., Wee, S., Rhee, E., Naumann, M., Dubiel, W. and Wolf, D.A. (2003) Fission yeast COP9/signalosome suppresses cullin activity through recruitment of the deubiquitylating enzyme Ubp12p. *Mol. Cell*, **11**, 927–938.

Accession numbers: GenBank accession numbers: pN-TAPa (AY788908), pC-TAPa (deposited as pYL436; AY737283).